Gernod Deckelmann (Autor)
Rosa Espinosa-Marzal (Autor)
Lutz Franke (Autor)

Simulation of Time Dependent Degradation of Porous Materials

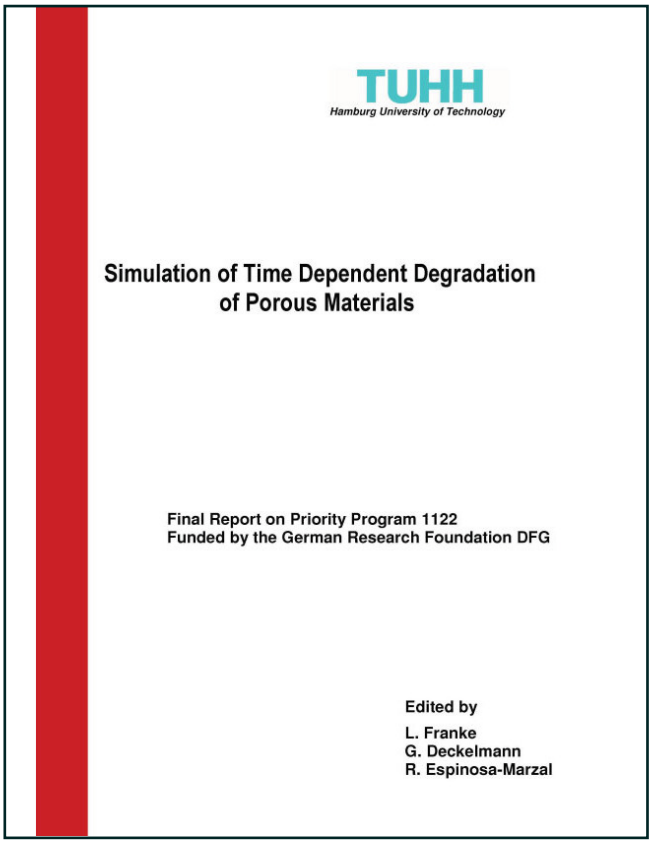

https://cuvillier.de/de/shop/publications/1159

Matthias Koster
Dr.-Ing. Dipl. Phys.

Wolfgang Brameshuber
Univ.-Prof. Dr.-Ing.

Institute of Building Materials Research (ibac), RWTH Aachen University, Aachen, Germany

Simulation of the Microstructure of Cement-Based Materials
- 3D-Simulation of Moisture Transport -

Summary

The research project focuses on simulating the moisture transport processes permeation, diffusion and capillary absorption in hardened cement pastes and mortars as the first two scale levels of a multi-scale model for describing the hygric properties of concrete. On the basis of three-dimensional representations of the microstructure of the hardened cement pastes and the mortars the various moisture transport coefficients are calculated with finite element methods. The generation of a moisture distribution in the materials serves as a prerequisite for simulating frost attack of concrete tackled by a companion project.

Keywords: *moisture transport, hardened cement paste, mortar, permeation, diffusion, capillary absorption, finite element method*

1 Introduction

The durability of porous building materials is significantly affected by their capabilities to transport moisture. This results from the fact that most of the damaging reagents (e.g. sulphates, chlorides) enter the material solved in water or by the so-called “piggyback transport”. The prediction of the durability of the building materials is therefore closely connected to the question of their hygric properties. This is especially true for the damaging of concrete due to frost which was the subject of the cooperation of the Institute of Building Materials Research, RWTH Aachen University (ibac) and the Institute of Mechanics and Computational Mechanics, Leibniz University Hannover (ibnm). The part of the project dealt with at the ibac encompass the simulation of moisture transport and the derivation of the hygric material properties whereas the ibnm was engaged in the mechanical modeling with the goal to deduce the mechanical properties of the materials and to simulate the arising stresses due to frost attack.

Since the building material “concrete” covers several length scales starting from the nano level of the gel phases up to the macro level of the construction component, the limited computational power of today’s data processing equipments prohibits the use of one all-encompassing model. In fact, multi-scale models have to be used to capture the complex nature of concrete. The workings so far dealt with the micro level of the hardened cement paste (typical length scale:

100 µm) and the meso level of the mortar (typical length scale: 10 mm) representing the first steps towards a multi-scale model of concrete.

The approach chosen aimed for calculating the hygric and mechanical properties of hardened cement pastes and mortars on the basis of three-dimensional representations of their microstructure without further assumptions or empirical parameters that would have to be determined experimentally.

In the following the generation of the 3D microstructure of the materials and the simulation of the moisture transport are presented. The transport processes considered encompass the water vapor diffusion, the water permeation and the capillary absorption in hardened cement pastes and mortars. The overall procedure with respect to hardened cement pastes and sandstones is described in detail in [1], [2] .

2 Generation of the 3D microstructures of the hardened cement pastes

The first step of the simulation of moisture transport at the micro level of the multi-scale model of concrete consists in generating a three-dimensional representation of the microstructure of the hardened cement pastes which serves as basis for the later calculations. This aim is achieved by two ways: Firstly, by using the simulation software CEMHYD3D ([3][4]), and secondly, by generating microtomographic images on the basis of the real material.

2.1 Used cements

The base material for the hardened cement pastes was a micro-milled Portland cement with a median grain size d_{50} of approximately 3.4 µm and a Blaine value of 10300 cm^2/g. A fine-ground cement was used in order to keep the representative volume element for the simulation with CEMHYD3D as small as possible in order to reduce the computational power needed. Furthermore, since in CEMHYD3D no diffusion through a closed surface of hydration products is implemented, smaller cement grains are able to hydrate up to a higher degree than larger grains.
The production and preparation of the samples for the microtomographic images (cf. Sect. 2.3) is described in [5].

2.2 Simulation of the microstructure of the hardened cement paste with CEMHYD3D

The computer program CEMHYD3D simulates the development of a three-dimensional microstructure of Portland cement with time during hydration. The software was developed by Bentz et al. at the National Institute of Standards and Technology (NIST), USA.

Starting from SEM (scanning electron microscopy) images of the cement powder, its particle size distribution, and the selected water to cement ratio a three-dimensional computational model of the cement paste is generated by CEMHYD3D. On the basis of this 3D model the hy-

dration of the cement paste is simulated. At the end of the procedure a three-dimensional computational model of the hardened cement paste (hcp) is generated. Two hardened cement pastes were simulated. Their water to cement ratios and degrees of hydration are shown in Table 1.

Table 1: Water to cement ratios w/c and degrees of hydration α of the hardened cement pastes

Name	**w/c**	α
hcp-45	0.45	0.95
hcp-55	0.55	0.99

The initial microstructure of the cement paste generated with CEMHYD3D and the resulting microstructure of the hardened cement paste for the hcp-45 are displayed in Figure 1. The side length of the microstructures amounts to 256 voxels with a voxel length of 1 µm.

(a) Initial cement paste microstructure (b) Hardened cement paste (hcp-45)

Figure 1: Initial 3D microstructure of the cement paste and simulated hardened cement paste (hcp-45)

2.3 Microtomographic images of the hardened cement pastes

In order to decide whether the simulated microstructures are realistic microtomographic images of real hcp samples with a resolution of about 1 µm/voxel were made. After acquisition of the microtomographic data sets, noise was removed by applying a median filter. Subsequently, the microtomographic images were segmented in unhydrated clinker phases, hydration products and pores by thresholding, making use of the cement hydration model of Powers [6]. The microtomographic images of both hardened cement pastes hcp-45 and hcp-55 are depicted in Figure 2.

(a) hcp-45 (b) hcp-55

Figure 2: µCT images of the hardened cement pastes hcp-45 and hcp-55 after segmentation

2.4 Rescaling of the resolution of the microstructures

Both the microstructures simulated with CEMHYD3D and the microtomographic images of the hardened cement pastes have a resolution of about 1 µm/voxel. Hence the submicron part of the pore space, which is significant for the moisture transport, is not captured. In Figure 3 the results of the mercury intrusion porosimetry (MIP) of the hcp-45 are shown.

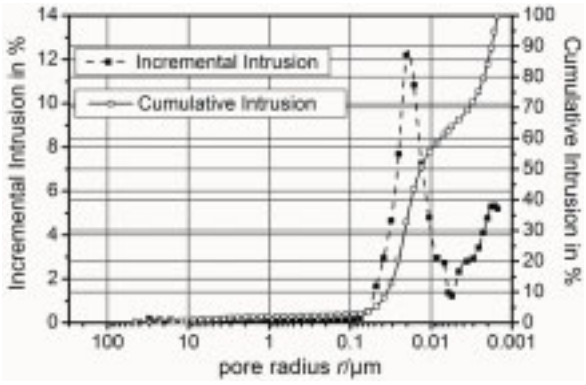

Figure 3: MIP curves of the hcp-45

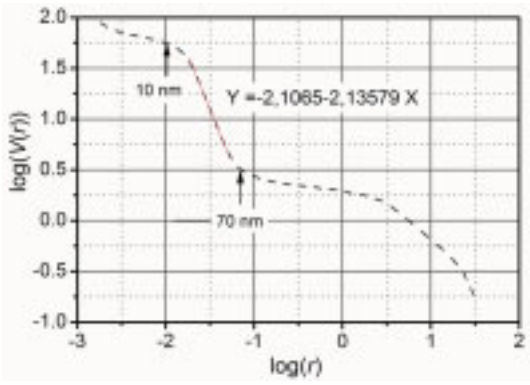

Figure 4: log(V(r)-log(r) plot of the cumulative MIP curve of the hcp-45

According to [7], pores with radii larger than the critical radius r_c, defined by the inflection point of the cumulative intrusion curve, do not form a connected network but are linked by smaller pore channels which act as bottle necks with respect to moisture transport. The critical radii of the hardened cement pastes cover a range between 10 nm and 30 nm. In Figure 4 the log(V(r))-log(r) plot of the cumulative MIP curve in Figure 3 is displayed. Linear segments of the curve represent domains of self-similarity with a fractal dimension defined by the slope of the segment. In case of the hcp-45 the fractal dimension amounts to 2.14 in the range of r_c. The pore space of the corresponding microtomographic image of the hcp-45 also is self-similar with a fractal dimension of 2.12, calculated with a three-dimensional version of the box-counting method described in [8]. Due to the self-similarity of the pore space and accounting for the fact that the fractal dimension of the pore space of the microtomographic image is almost identical to that

of the real material the resolution of the simulated microstructures and the microtomographic data sets was scaled up to 20 nm/voxel assuming that pores with a smaller radius only make a minor contribution to the overall moisture transport.

The change of the resolution scale only affects the later simulation of the permeation and the capillary absorption. The diffusion is independent of the resolution.

3 Simulation of the moisture transport in the hardened cement pastes

The basic approach to simulate the moisture transport in the hardened cement pastes is to replace their pore spaces with networks of cylindrical tubes which possess the same moisture transport properties. On the basis of the transportation networks the moisture transport coefficients are calculated using finite element methods.

3.1 Generating of the moisture transport networks of the hardened cement pastes

The first step in generating the moisture transport networks consists in extracting the medial axis of the pore spaces of hardened cement pastes. This is achieved by a modified version of the “thinning algorithm” described in [9]: Starting with the solid – pore interface all pore voxels that fulfill certain adjacency relations to their neighbor voxels are deleted until the medial axis remains. In a second step all dead end branches and isolated parts of the medial axis, i.e. parts that are not linked to the surface of the microstructures, are removed. Afterwards all voxels where branches of the medial axis intersect are identified using the concept of λ-adjacency [10].

The transportation network is generated by replacing all branches of the medial axis by cylindrical tubes having the same moisture transport properties than the original pore channels. The starting and end points of the tubes are marked by the previously determined intersection points of the medial axis branches.

The diameters of the tubes are assigned in the following way: Each voxel of the medial axis is considered as center point of a sphere, which is steadily increased until it contacts the solid phase. The resulting radius of the sphere is afterwards assigned to the center voxel.

In case of simulating the water permeation the effective hydraulic radius of the pore channels enters the corresponding equations. The hydraulic radius for each voxel of the medial axis is determined by the area A and the perimeter P of the pore channel perpendicular to the medial axis through this voxel, according to

$$r_H = 2\frac{A}{P}. \tag{1}$$

Having assigned a diameter, the voxels of the medial axis are considered as small tubes. The radius of a tube in the transportation network then follows from the calculation of the radius of a serial connection of one voxel long tubes, namely the voxels of the medial axis it consists of.

In Figure 5 a part of the medial axis and the resulting transportation network of the pore space of the microtomographic data set of the hcp-45 are shown.

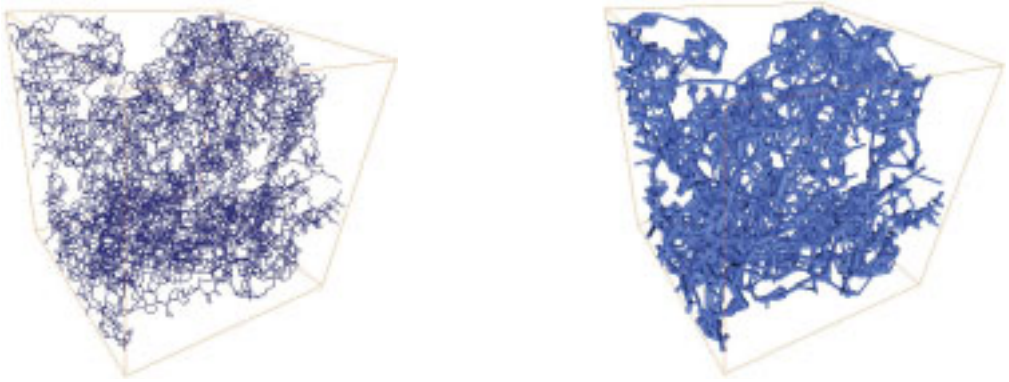

Figure 5: Medial axis and resulting transportation network of the pore space of the µCT image of the hcp-45 (the side length of the displayed volumes is 128 µm)

After generating of the transportation networks the different moisture transport processes (diffusion, permeation and capillary absorption) are simulated with finite element methods.

3.2 Water vapor diffusion of the hardened cement pastes

The simulation of the water vapor diffusion in the hardened cement pastes is carried out by replacing every tube of the transportation networks by one-dimensional heat conducting elements. The mass flow rate in a tube t_{ij} ranging from node i to node j is calculated by Fick's first law, i.e.

$$Q_{ij} = D_{air} \cdot A_{ij} \cdot \frac{\Delta c_{ij}}{L_{ij}} \tag{2}$$

where D_{air} is the diffusion coefficient of water vapor in air, A_{ij} is the cross section of the tube, L_{ij} its length and $\Delta c_{ij} = c_i - c_j$ the imposed water vapor concentration difference. Since the t_{ij} are serial connections of n one voxel long tubes the relations

$$\begin{aligned} Q_{ij} &= Q_k \\ \Delta c_{ij} &= \sum_{k=1}^{n} \Delta c_k \end{aligned} \tag{3}$$

hold. From Eqs. (2) and (3) the diameter of t_{ij} is calculated by

$$d_{ij} = \sqrt{\frac{L_{ij}}{\sum_{k=1}^{n} \frac{L_k}{d_k^2}}} \,. \tag{4}$$

The total mass flow rate within the microstructure is given by

$$Q = D_{hcp} \cdot A \cdot \frac{\Delta c}{L} = \sum_{j \in A_{out}} Q_{ij} \tag{5}$$

with D_{hcp} denoting the water vapor diffusion coefficient of the hardened cement paste, A the cross section, and L the length of the volume passed through by the water vapor, and Δc the imposed vapor concentration difference between inlet and outlet surface of the volume. Constant concentration boundary conditions were used for all nodes and no-flow boundary conditions for all end nodes of tubes not lying on the inlet or outlet surface. The mass flow rate within the porous medium is calculated by summation of the mass flow rates of all tubes crossing the outlet surface. The simulated water vapor diffusion coefficients of both hardened cement pastes are shown in Table 2. The degree of compliance between the water vapor coefficients of the microtomographic images and those of the simulated microstructures depends on the water to cement ratio, as can be seen from Table 2.

Table 2: Simulated water vapor diffusion coefficients of the hardened cement pastes

Hardened cement paste	**D_{hcp}**	
	µCT	**CEMHYD3D**
	10^{-7} m^2/s	
hcp-45	0.8	7.1
hcp-55	16.1	12.4

Unfortunately the water vapor diffusion coefficients of the hardened cement pastes could not be determined experimentally due to a pronounced tendency to form drying shrinkage cracks. For comparison experimental results of a hardened cement paste consisting of an ordinary Portland cement according to [11] are displayed in Table 3.

Table 3: Measured water vapor diffusion coefficients of hardened cement pastes made of ordinary Portland cement

w/z	**D_{hcp}**
	10^{-7} m^2/s
0.35	2.2
0.45	4.1
0.60	6.1

Even though, the water vapor diffusion coefficients of Table 3 cannot be compared directly to those in Table 2, because of different raw materials, the values lie in the same order of magnitude.